

Renormalizing the gauged Wess-Zumino-Witten Lagrangian to one loop in a one-family technicolor model

David H. Slaven* and Bing-Lin Young

Ames Laboratory and Department of Physics, Iowa State University, Ames, Iowa 50011

(Received 6 May 1991)

We examine the problems of calculating processes to one loop in a Wess-Zumino-Witten model, using one-family technicolor as an example and gauging the QCD subgroup of the chiral symmetry of technifermions. In particular, we examine decay processes of certain technipions, often denoted P^0 and P_8^0 . We find that almost all of the ultraviolet divergences cancel. The cancellation of infrared divergences between processes with degenerate final states provides us with a constraint on our renormalization scheme. We also study the effects of different d -dimensional prescriptions for $\epsilon^{\mu\nu\alpha\beta}$ and γ_5 in dimensional regularization. (The matrix γ_5 appears when we include possible extended technicolor couplings between technipions and ordinary fermions.) In the end, we choose $\overline{\text{MS}}$ renormalization, and a noncovariant prescription for $\epsilon^{\mu\nu\alpha\beta}$ and γ_5 . We also present one-loop corrections to the width of the P^0 . These turn out to be sizable.

PACS number(s): 12.15.-y, 11.10.Gh, 11.15.Ex

I. INTRODUCTION

The Wess-Zumino-Witten Lagrangian [1,2] is an effective Lagrangian used in describing the low-energy behavior of Nambu-Goldstone bosons in a confining theory of fermions, such as QCD. This piece of the full effective Lagrangian arises from an Adler-Bell-Jackiw anomaly in the fermion currents of the underlying fundamental theory. While Wess, Zumino, Witten, and others have used this Lagrangian to describe low-energy QCD, we can also use it to describe the low-energy behavior in a technicolor [3] theory.

The gauge group of QCD, $SU(3)_c$, is a flavor subgroup of the chiral symmetry of the technifermions in technicolor. We can gauge this subgroup [2,4] in order to include ordinary strong interactions in our Lagrangian. This will give us interactions between technipions and gluons. These couplings will be largely responsible for the decays of technipions.

We will be dealing with a one-family technicolor model of Farhi and Susskind [3], and so the spectrum of technifermions consists of an isodoublet of techniquarks, which come in three colors, and an isodoublet of colorless technileptons. [The left-handed components of these isodoublets are $SU(2)_L$ doublets, while the right-handed components are singlets.] There are 60 technipions in such a model. The lightest technipion is expected to be a colorless, neutral, weak-isosinglet particle, often denoted P^0 . We have studied this particle before [5] and found that the lowest-order decays are not as dominant as was previously expected. In particular, we found that three-body decays which are QCD corrections to two-body decays are comparable to the lowest-order two-body decays.

In addition, we found that these same corrections led to an enhancement of P^0 production at hadron colliders.

In considering the three-body decays, however, we neglected QCD corrections to the two-body decays which are of the same order in α_s . These corrections to the two-body decays involve products of the tree-level diagrams with one-loop, ultraviolet-divergent diagrams, and they are the focus of this work.

In addition to the Wess-Zumino-Witten Lagrangian, we also consider the effects of an extended technicolor [6] interaction (or some other interaction) which couples technipions to ordinary fermions. In most extended technicolor models, the couplings of technipions to ordinary fermions is proportional to the fermion mass. We will work under this assumption, and this will affect our renormalization.

In Sec. II we explain our renormalization procedure. Section III exhibits the problems of mass singularities and shows how we separate the ultraviolet and infrared divergences. We describe and justify our procedure for handling the Levi-Civita tensor and γ_5 in Sec. IV. These are two objects which are inherently four dimensional, and when we use dimensional regularization, there is no satisfying prescription for continuing these objects to d dimensions. In Sec. V, we show the cancellation of most of the ultraviolet divergences. This is not trivial, since we are not dealing with a renormalizable theory. We present the results of calculations with the P^0 in Secs. VI and VII and follow this with a short conclusion. An Appendix contains details of how the phase-space integration was performed.

II. RENORMALIZING THE EFFECTIVE LAGRANGIAN

The effective Lagrangian we will be using here is a non-renormalizable model, and as a result, we will not be able to renormalize to all orders. We will be content to renormalize just to lowest order in QCD. In order to calculate

*Current address: Department of Physics and Astronomy, Drake University, Des Moines, IA 50311.

the $O(\alpha_s)$ corrections to two-body decays, we must consider two-body decay diagrams that are just $O(\alpha_s)$ higher than tree-level two-body diagrams. This will usually (though not always) be equivalent to considering one-loop diagrams.

Since we have coupled the effective Lagrangian to QCD, we begin our renormalization by renormalizing QCD. We choose the gauge-invariant method of dimensional regularization for regularizing both the ultraviolet and infrared divergences. One of our first choices to make is that of a renormalization scheme. It has been shown [7,8] that on-shell renormalization is inappropriate for QCD. When one renormalizes the coupling constant in an on-shell scheme, the cancellation of infrared divergences is spoiled by the infrared divergence in the coupling renormalization constant. Hence we will renormalize QCD by modified minimal subtraction ($\overline{\text{MS}}$). Our notation and the renormalization constants are presented in Table I.

Before we close the subject of subtraction scheme, however, we should briefly discuss one of the side effects of $\overline{\text{MS}}$. In the dimensional regularization scheme, ultraviolet divergences show up in the form

$$\frac{1}{\epsilon} - \gamma_E + \ln 4\pi + \ln \frac{\mu^2}{\tilde{M}^2}, \quad (1)$$

where μ is the renormalization scale and \tilde{M} is another mass scale relevant to the diagram being calculated (for example, the mass of one of the particles). Subtraction according to the $\overline{\text{MS}}$ scheme leaves the last term in (1). In the end we have a dependence on μ , a parameter with no physical significance.

A way around this problem would be to subtract the μ -dependent term along with the divergence. This implies including a second mass scale in the subtraction (to keep the argument of the logarithm dimensionless) such

TABLE I. Definition of the renormalization constants (left column) and their values. g is the QCD coupling constant, ψ and m denote any fermion field and its mass, G_μ^a is a gluon field, c^a is a ghost field, and ξ is the gauge parameter.

$g_0 = Z_g^{-1} g$	$Z_g = 1 + \frac{g^2}{(4\pi)^2} \left[\frac{11}{6} C_2(G) - \frac{2}{3} T(F) \right] \times \left[\frac{1}{\epsilon} - \gamma_E + \ln 4\pi \right]$
$\psi_0 = Z_2^{1/2} \psi$	$Z_2 = 1 - \frac{g^2 C_2(F)}{(4\pi)^2} \left[\frac{1}{\epsilon} - \gamma_E + \ln 4\pi \right]$
$G_{0\mu}^a = Z_3^{1/2} G_\mu^a$	$Z_3 = 1 + \frac{g^2}{(4\pi)^2} \left[\frac{5}{3} C_2(G) - \frac{4}{3} T(F) \right] \times \left[\frac{1}{\epsilon} - \gamma_E + \ln 4\pi \right]$
$c_0^a = Z_4^{1/2} c^a$	$Z_4 = 1 + \frac{g^2 C_2(G)}{(4\pi)^2} \frac{1}{2} \left[\frac{1}{\epsilon} - \gamma_E + \ln 4\pi \right]$
$\xi_0 = Z_5 \xi$	$Z_5 = Z_3$
$m_0 = m + \delta m$	$\delta m = - \frac{3g^2 C_2(F)}{(4\pi)^2} m \left[\frac{1}{\epsilon} - \gamma_E + \ln 4\pi \right]$

as \tilde{M} . This is akin to what one does in, for example, on-shell renormalization. In our calculation the mass that often turns up in the role of \tilde{M} in (1) is M , the mass of the P^0 . Performing the subtraction in this manner, however, is mathematically equivalent to performing strict $\overline{\text{MS}}$ and choosing $\mu = M$. We opt for strict $\overline{\text{MS}}$, leaving the effects of this choice of scale completely visible in the final result, so that the effect can be easily investigated. Later, we will show that varying μ by a factor of 2 up or down from $\mu = M$ changes the total of our corrections by a few percent for low P^0 mass, to just under 10% for $M = 150$ GeV.

Our next step is to extract the parts of the effective Lagrangian that we need. In our past works [5], we have concentrated on the P^0 and P_8^0 . We have chosen neutral isosinglet particles, since these are expected to be the particles that can most easily be produced singly in hadron colliders. Here we continue to concentrate on these particles. The terms in our effective Lagrangian which govern the interactions of the P^0 and P_8^0 with gluons are

$$\mathcal{L} = \frac{1}{2} (D_\mu \phi_8^a)^2 - \frac{N_{\text{TC}} \alpha_s}{4\pi F_\pi} \left[\frac{1}{4\sqrt{3}} \phi G_{\mu\nu}^a \tilde{G}^{a\mu\nu} + \frac{1}{2\sqrt{2}} d^{abc} \phi_8^a G_{\mu\nu}^b \tilde{G}^{c\mu\nu} \right]. \quad (2)$$

In (2), ϕ and ϕ_8^a are the P^0 and P_8^0 fields, respectively. D_μ is a covariant derivative defined by

$$D_\mu \phi_8^a = \partial_\mu \phi_8^a - g f^{abc} G_\mu^b \phi_8^c. \quad (3)$$

G_μ^a is the gluon field, $G_{\mu\nu}^a = \partial_\mu G_\nu^a - \partial_\nu G_\mu^a - g f^{abc} G_\mu^b G_\nu^c$, and we define $\tilde{G}^{a\mu\nu} = \epsilon^{\mu\nu\alpha\beta} G_{\alpha\beta}^a$. The constants f^{abc} and d^{abc} are the antisymmetric and symmetric structure constants of SU(3), respectively. N_{TC} is the number of technicolors [i.e., we assume technicolor is an SU(N_{TC}) gauge theory], g is the QCD coupling constant, $\alpha_s = g^2/4\pi$, and F_π is the technipion decay constant, 125 GeV for one-family technicolor. The first term of (2) is from the ordinary part of the effective Lagrangian, while the rest is from the Wess-Zumino-Witten Lagrangian. The Feynman rules from this Lagrangian are shown in Table II.

The Lagrangian containing (2) can be derived solely from symmetry considerations and topology. Since no

TABLE II. Feynman rules for interactions involving the P^0 and P_8^0 .

Vertex	Rule
$P^0 gg$	$2i \Gamma \epsilon^{\mu\nu\alpha\beta} \delta^{ab} k_{1\alpha} k_{2\beta}$
$P^0 ggg$	$-2g \Gamma \epsilon^{\mu\nu\alpha\beta} f^{abc} (k_1 + k_2 + k_3)_\mu$
$P_8^0 P_8^0 g$	$-g f^{abc} (k_2 - k_1)_\mu$
$P_8^0 P_8^0 gg$	$ig^2 g_{\mu\nu} (f^{abe} f^{cde} + f^{ade} f^{cbe})$
$P_8^0 gg$	$2i \Gamma' \epsilon^{\mu\nu\alpha\beta} d^{abc} k_{1\alpha} k_{2\beta}$
$P_8^0 ggg$	$-2g \Gamma' \epsilon^{\mu\nu\alpha\beta} (d^{abe} f^{cde} k_{1\mu} + d^{ace} f^{bde} k_{2\mu} + d^{ade} f^{bce} k_{3\mu})$
$P_8^0 gggg$	$2ig^2 \Gamma' \epsilon^{\mu\nu\alpha\beta} d^{afg} (f^{bcf} f^{deg} + f^{bdf} f^{ecg} + f^{bef} f^{cdg})$
$P^0 ff$	$-G \gamma_5$
$P_8^0 \bar{q}q$	$-G_8 T^a \gamma_5$

perturbation theory or renormalization is done in arriving at this, the quantities in (2) are bare quantities. We will be doing a perturbative calculation in the renormalized quantities, and so we need to express (2) in terms of renormalized quantities. This can be done with the help of the information in Table I.

For example, one of the terms in our Lagrangian is

$$-\frac{N_{\text{TC}}g_\eta^2}{16\sqrt{3}\pi^2F_\pi}\epsilon^{\mu\nu\alpha\beta}\phi_0(\partial_\mu G_{0\nu}^a)(\partial_\alpha G_{0\beta}^a), \quad (4)$$

where the zeros on the coupling and fields show that these are bare quantities. Before we replace the bare fields, we must first see if the $P^{0'}$ field undergoes any renormalization due to propagator corrections from QCD. The lowest-order correction is shown in Fig. 1. This diagram, however, is a correction of order $O(\alpha_s^2)$, which is higher order than we wish to consider here. Therefore we ignore this, and to lowest order the $P^{0'}$ propagator is unrenormalized.

Knowing this, we can replace the bare quantities with renormalized quantities, and (4) becomes

$$-\frac{N_{\text{TC}}g^2}{16\sqrt{3}\pi^2F_\pi}\epsilon^{\mu\nu\alpha\beta}\phi(\partial_\mu G_\nu^a)(\partial_\alpha G_\beta^a)Z_g^{-2}Z_3. \quad (5)$$

Expanding the renormalization constants in (5), we get

$$-\frac{N_{\text{TC}}g^2}{16\sqrt{3}\pi^2F_\pi}\epsilon^{\mu\nu\alpha\beta}\phi(\partial_\mu G_\nu^a)(\partial_\alpha G_\beta^a) \times \left[1 - \frac{2\alpha_s C_2(G)}{4\pi} \left(\frac{1}{\epsilon} - \gamma_E + \ln 4\pi \right) \right], \quad (6)$$

where $C_2(G)$ is the second-order Casimir invariant for the adjoint representation of the gauge group [3 for $\text{SU}(3)_c$], γ_E is Euler's constant, and ϵ is $2-d/2$, where d is the number of space-time dimensions in dimensional regularization. In the four-dimensional limit, $\epsilon \rightarrow 0$. The first term reproduces the tree-level Feynman rule, while the second term is a counterterm that must be included among our corrections.

We can do the same thing for the $P_8^{0'}$. This case is only slightly different because of the color of the $P_8^{0'}$. In particular, the corrections to the $P_8^{0'}$ propagator, shown in Fig. 2, are $O(\alpha_s)$, and so we must consider these diagrams as well. The loop integral in the second diagram of Fig. 2 is the same as that in the correction to the gluon propagator involving the four-gluon vertex, and so it is defined to vanish. The first one, however, is ultraviolet divergent and forces us to renormalize the $P_8^{0'}$ propagator. This gives us a new renormalization constant



FIG. 1. Propagator correction to $P^{0'}$.



FIG. 2. Propagator correction to $P_8^{0'}$.

$$\begin{aligned} \phi_{8_0}^a &= Z_8^{1/2} \phi_8^a, \\ Z_8 &= 1 + \frac{2g^2 C_2(G)}{(4\pi)^2} \left[\frac{1}{\epsilon} - \gamma_E + \ln 4\pi \right]. \end{aligned} \quad (7)$$

This new renormalization constant must be taken into account when we substitute the renormalized fields for the bare fields and obtain the counterterms.

Next, we include the possibility of extended technicolor (ETC) interactions in our effective Lagrangian. ETC is an interaction introduced to give masses to ordinary fermions. It gives the fermions mass by coupling them to the technicolor vacuum condensate. For this reason the couplings of technifermions, and hence technipions, to an ordinary fermion are assumed to be proportional to the fermion's mass. With this in mind, we couple our technipions to ordinary fermions by

$$\mathcal{L}_{\text{ETC}} = \sum_j (iG_f \phi \bar{\psi} \gamma_5 \psi + iG_{8f} \phi_8^a \bar{\psi} \gamma_5 T^a \psi), \quad (8)$$

where the sum is over all flavors of fermions (quarks only for the $P_8^{0'}$) and the γ_5 is for parity conservation. We do not include flavor-changing neutral-current interactions here. The constant G_f is of the form

$$G_f = C_f \frac{m_f}{F_\pi}, \quad (9)$$

where m_f is the mass of the ordinary fermion and C_f is some constant (~ 1), which can vary from one flavor to the next. G_{8f} has the same form.

When we renormalize we have the same situation we had for the Wess-Zumino-Witten Lagrangian. We again replace the bare quantities with the renormalized quantities. For the first term we get

$$iG_{f0} \phi_0 \bar{\psi}_0 \gamma_5 \psi_0 = iG_f \left[1 + \frac{\delta m}{m} \right] Z_2 \phi \bar{\psi} \gamma_5 \psi. \quad (10)$$

The factor $1 + \delta m/m$ comes when we replace the bare mass in the constant G_f with the renormalized mass. The second term in (8) gives us a similar expression, except that we must include the factor $Z_8^{1/2}$ for the $P_8^{0'}$ field renormalization. The end result of this is again the tree-level Feynman rule plus a counterterm.

III. PROBLEM OF MASS SINGULARITIES

Mass singularities must be handled specially because there is a problem in separating the ultraviolet from the infrared divergences. To illustrate the situation and demonstrate how we handle it [8], we examine briefly the case of the gluon loop corrections to the gluon propagator. This is given by

$$\Pi^g(k^2) = \frac{g^2 C_2(G)}{(4\pi)^2} \frac{5}{3} \left[\frac{1}{\varepsilon} - \gamma_E + \ln 4\pi + \frac{31}{15} \right] \left[\frac{-k^2}{\mu^2} \right]^{-\varepsilon}, \quad (11)$$

where the superscript g expresses the fact that we have only included the gluon contribution and we have expanded some of the factors in ε . The problem is in the last factor. If $\varepsilon = 2 - d/2$ is positive, then this factor is undefined as we go on the mass shell ($k^2 = 0$). But $\varepsilon > 0$ is the appropriate condition for regularizing ultraviolet divergences.

We begin by renormalizing in the $\overline{\text{MS}}$ scheme, with the gluon off shell. This means that we subtract

$$\Pi_{\bar{g}}^g = \frac{g^2 C_2(G)}{(4\pi)^2} \frac{5}{3} \left[\frac{1}{\varepsilon} - \gamma_E + \ln 4\pi \right]. \quad (12)$$

Then, for our renormalized propagator correction, we get

$$\begin{aligned} \Pi_{\bar{g}}^g(k^2) &= \Pi^g(k^2) - \Pi_{\bar{g}}^g \\ &= \frac{g^2 C_2(G)}{(4\pi)^2} \frac{5}{3} \left[\left[\frac{1}{\varepsilon_i} - \gamma_E + \ln 4\pi \right] \right. \\ &\quad \times \left[\left[\frac{-k^2}{\mu^2} \right]^{-\varepsilon_i} - 1 \right] \\ &\quad \left. + \frac{31}{15} \left[\frac{-k^2}{\mu^2} \right]^{-\varepsilon_i} \right]. \quad (13) \end{aligned}$$

For $k^2 \neq 0$ expression (13) is convergent in the limit $\varepsilon \rightarrow 0$. Therefore we have removed the ultraviolet divergence. Any remaining divergence must be infrared, and so we are justified in using the subscript i on the ε 's of (13). Since we no longer need to regularize the ultraviolet, we can now take $\varepsilon_i < 0$. This is the appropriate condition for regularizing infrared divergences. Once we do this, we can go on shell. As $k^2 \rightarrow 0$, $(-k^2/\mu^2)^{-\varepsilon_i} \rightarrow 0$, so that

$$\Pi_{\bar{g}}^g(0) = -\frac{g^2 C_2(G)}{(4\pi)^2} \frac{5}{3} \left[\frac{1}{\varepsilon_i} - \gamma_E + \ln 4\pi \right]. \quad (14)$$

Now the infrared divergence is apparent.

IV. LEVI-CIVITA TENSOR AND γ_5

We have chosen for our regularization scheme the gauge-invariant method of dimensional regularization. There are, however, some ambiguities that we must address before we can actually calculate any physical processes. These ambiguities in dimensional regularization involve the inherently four-dimensional quantities $\epsilon^{\mu\nu\alpha\beta}$ and γ_5 . The treatment of these two objects has been a subject of debate since the inception of dimensional regularization.

The study of the Levi-Civita tensor which is most relevant to our work is by Bos [9]. Bos works with the Wess-Zumino-Witten model in two space-time dimensions, a model in which many quantities can be calculated exactly. Some of these exact results involve relationships

between renormalization-group coefficients. Bos takes some of these exact relations and rederives them perturbatively, using both a covariant prescription and a strictly two-dimensional prescription for the Levi-Civita tensor. The noncovariant (two-dimensional) prescription consists of stating that

$$\epsilon^{\mu\nu} = 0 \quad \text{whenever } \{\mu, \nu\} \neq \{0, 1\}. \quad (15)$$

The other components are the same in d dimensions as in two. The Lorentz-covariant prescription amounts to declaring the indices to be antisymmetric and taking

$$\epsilon^{\mu\nu} \epsilon^{\alpha\beta} = -F(d)(g^{\mu\alpha} g^{\nu\beta} - g^{\mu\beta} g^{\nu\alpha}), \quad (16)$$

where $F(d)$ is an analytic function and $F(2) = 1$. One should note that this constraint is not completely consistent. For example, in evaluating the quantity

$$\epsilon^{\mu\nu} \epsilon^{\rho\sigma} \epsilon_{\nu\rho}, \quad (17)$$

one can use (16) on either the first two tensors or the last two tensors. If one demands the same result in each case, one must require $(d-2)F(d) = 0$. This would imply that $F(d) = 0$ whenever $d \neq 2$. Coupled with our requirement that $F(2) = 1$, we see that one cannot smoothly take the limit $d \rightarrow 2$ as required in dimensional regularization. This same inconsistency lurks in the analogous four-dimensional case. If one does not encounter expressions such as (17), however, then this may not be a problem.

Bos finds that the two-dimensional tensor (15) reproduces the exact result order by order, while the covariant tensor (16) fails. Since we have no better constraint than this, we will use a strictly four-dimensional definition of the d -dimensional $\epsilon^{\mu\nu\alpha\beta}$, although we will perform some of our calculation using both prescriptions for comparison.

Since $\epsilon^{\mu\nu\alpha\beta}$ and γ_5 are related objects, we will also use a noncovariant prescription for γ_5 to be consistent. This is defined by

$$\gamma_5 = i\gamma^0\gamma^1\gamma^2\gamma^3, \quad (18)$$

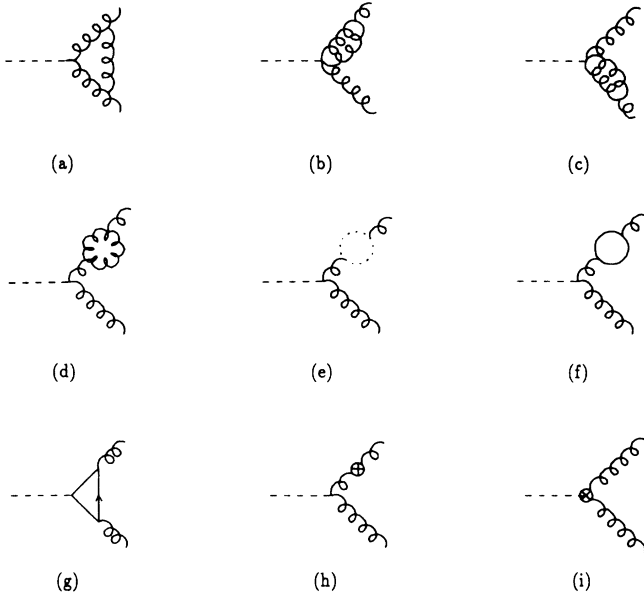
which will lead to the mixed commutation relations

$$\{\gamma_5, \gamma_\mu\} = 0, \quad \mu = 0, 1, 2, \text{ or } 3, \quad (19)$$

$$[\gamma_5, \gamma_\mu] = 0, \quad \mu > 3.$$

The Lorentz noncovariance of these inherently four-dimensional objects will make the calculation very complicated, but our best indication (Bos) is that this is the best way to proceed.

Along with γ_5 and $\epsilon^{\mu\nu\alpha\beta}$, we must decide how to extend the external momenta to d dimensions. It is common in renormalization to take the external momenta to be strictly four-dimensional objects; that is, all components are zero except the first four. This is not appropriate, however, in our case. Two of the processes we shall be dealing with are the decays $P^{0'} \rightarrow gg$ and $P^{0'} \rightarrow ggg$. The Feynman diagrams for these processes are shown in Figs. 3 and 4. There is an infrared divergence associated with each of these processes. In the three-gluon decay, the infrared divergence appears in the phase-space integral when one of the gluons is soft or two of them are col-

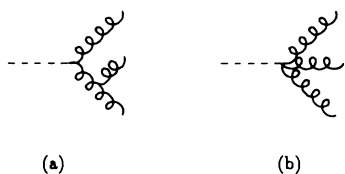
FIG. 3. Diagrams for the decay $P^0 \rightarrow gg$.

linear. In the two-gluon decay, the divergence arises in the loop integration when one of the internal gluons is on shell. When we regularize the divergences and add up the decay rates to these two processes, however, the infrared divergences between the two processes should cancel. There are two ways that we can regularize the infrared divergences. The first is to give the gluon a small mass. This is not a gauge-invariant method, however, and when we employ it we find that the infrared divergences between the two processes will not cancel. The other way is to use dimensional regularization for the infrared as well as the ultraviolet divergences. This method works; the infrared divergences cancel.

For the three-gluon case, this means that we perform the phase-space integral over d dimensions instead of four. Therefore our choice of regularization scheme for the infrared divergences leads us to take the external momenta to be d dimensional, and we cannot set the extra components of these to zero. For consistency, we treat the external momenta the same way (d dimensionally) for the two-gluon decay as well. We are now in a position to see how noncovariance complicates matters in the phase-space integrals.

All the two-body decay amplitudes are proportional to $\epsilon^{\mu\nu\alpha\beta} k_{1\alpha} k_{2\beta}$. When we square the amplitude, we get

$$\epsilon^{\mu\nu\alpha\beta} \epsilon_{\mu\nu\rho\sigma} k_{1\alpha} k_{2\beta} k_1^\rho k_2^\sigma, \quad (20)$$

FIG. 4. Diagrams for the decay $P^0 \rightarrow ggg$. There are two others found by permuting the gluons in (a).

where k_1 and k_2 are the gluon momenta. With a noncovariant $\epsilon^{\mu\nu\alpha\beta}$ tensor,

$$\epsilon^{\mu\nu\alpha\beta} \epsilon_{\mu\nu\rho\sigma} = -2(\underline{g}_{\rho\sigma} g_\alpha^\beta - \underline{g}_{\sigma\alpha} g_\rho^\beta), \quad (21)$$

where underlined quantities hereafter will denote quantities that are truncated to four dimensions. Then, for (20), we get

$$\epsilon^{\mu\nu\alpha\beta} \epsilon_{\mu\nu\rho\sigma} k_{1\alpha} k_{2\beta} k_1^\rho k_2^\sigma = -2[\underline{k}_1^2 \underline{k}_2^2 - (\underline{k}_1 \cdot \underline{k}_2)^2]. \quad (22)$$

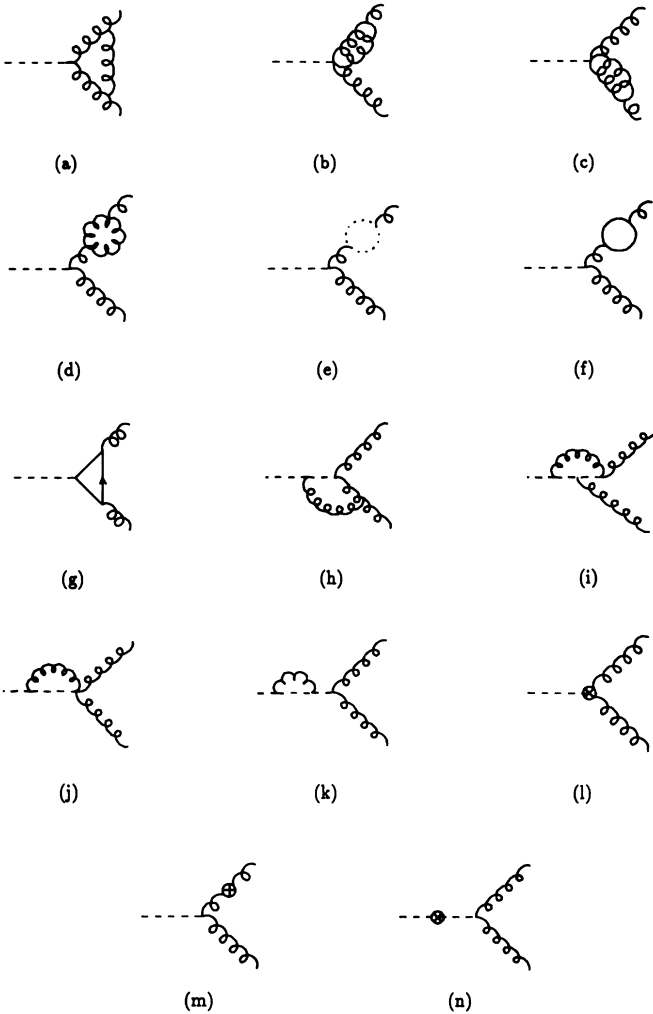
If we take k_μ to be a four-dimensional object, then $\underline{k}_1 \cdot \underline{k}_2 = k_1 \cdot k_2$ and $\underline{k}^2 = k^2 = 0$. If k_μ is a d -dimensional object, then $\underline{k}_1 \cdot \underline{k}_2 = k_1 \cdot k_2 + O(\epsilon)$, etc. Now we see that when we perform our phase-space integration, we no longer have a Lorentz-covariant integrand. Details of the phase-space integration are in the Appendix.

In the case of the ultraviolet divergences, the worst divergence we encounter goes as $1/\epsilon$. This means that using different conventions for $\epsilon^{\mu\nu\alpha\beta}$ or γ_5 will give us results that differ only in the finite part. This is because the differences in $\epsilon^{\mu\nu\alpha\beta}$ and γ_5 themselves will only be $O(\epsilon)$. The infrared case, however, is different. The worst infrared divergence is proportional to $1/\epsilon^2$. Therefore using different prescriptions for $\epsilon^{\mu\nu\alpha\beta}$ and γ_5 can lead to differences in the divergent part. One could imagine that these differences could spoil the infrared-divergence cancellation, and so we might find that one prescription works while the other one does not. In fact, this is not the case. Using either prescription for $\epsilon^{\mu\nu\alpha\beta}$ and γ_5 in an arbitrary number of dimensions results in the cancellation of infrared divergences, although the finite result differs in the two cases.

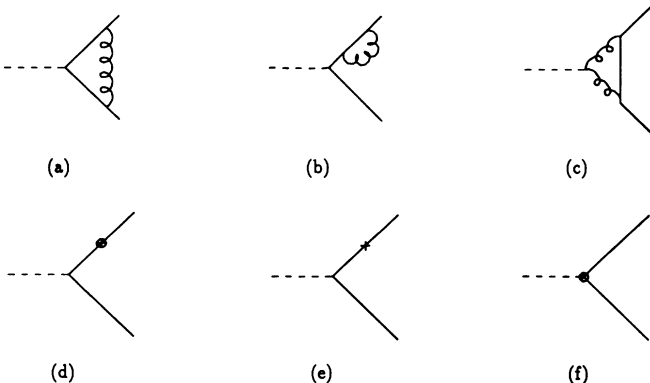
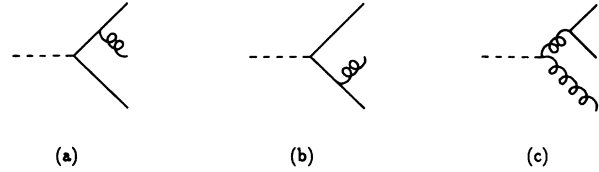
V. ULTRAVIOLET BEHAVIOR OF ONE-LOOP DIAGRAMS

Now we shall see how this renormalization affects the ultraviolet behavior of $P^0 \rightarrow gg$, $P_8^0 \rightarrow gg$, $P^0 \rightarrow \bar{q}q$, and $P_8^0 \rightarrow \bar{q}q$. The diagrams for some of these processes are shown in Figs. 3, 5, and 6. We begin with the first process. The ultraviolet divergences in diagrams of Figs. 3(d), 3(e), and 3(f) are, by design, canceled by the counterterm of Fig. 3(i). The divergences in Figs. 3(a)–3(c) are canceled by the counterterm of Fig. 3(i). This leaves only the diagram of Fig. 3(g), and this is finite. All the ultraviolet divergences in this process have canceled, and the result is ultraviolet finite. Although our cancellation here is presented in the Feynman gauge, this cancellation of ultraviolet divergences is, in fact, gauge invariant. If we had not treated the quantities in the Wess-Zumino-Witten Lagrangian as bare quantities, then we would not have had the counterterm of Fig. 3(i). Then we would have not only been left with ultraviolet divergences, but we would have obtained an answer that was gauge dependent. The ultraviolet divergences in the process $P_8^0 \rightarrow gg$ disappear in a completely analogous manner, the only difference being the correction to the P_8^0 propagator [Fig. 5(k)] and the counterterm [Fig. 5(n)] introduced to cancel its ultraviolet divergence.

The ultraviolet divergences in the quark decays of the P^0 and P_8^0 are not so well behaved. The ultraviolet

FIG. 5. Diagrams for the decay $P_8^0 \rightarrow gg$.

divergences from the quark-propagator correction of Fig. 6(b) is canceled by the counterterms of Figs. 6(d) and 6(e). The divergence from Fig. 6(a) is canceled by the counterterm of Fig. 6(f). We are left, however, with Fig. 6(c), which is a diagram with an ultraviolet divergence. There are no counterterms or other diagrams to cancel the ul-

FIG. 6. Diagrams for the decay $P^0 \rightarrow \bar{q}q$.FIG. 7. Diagrams for the decay $P^0 \rightarrow \bar{q}qg$.

traviolet divergence here, and so we have this divergence left over. The same thing happens in the decay $P_8^0 \rightarrow \bar{q}q$. In the end we are left with a divergent graph similar to Fig. 6(c).

For the diagrams which produce ultraviolet divergences which are not canceled, dimensional regularization is not an appropriate scheme. In this scheme we are left with our regularization parameter $\epsilon = 2 - d/2$, which should approach zero in the four-dimensional limit. Since this parameter has no physical significance, it is a bad parameter to have left at the end of the calculation. Therefore, for the diagram of Fig. 6(c), we impose an ultraviolet cutoff in the integral. The cutoff can be given a physical meaning. In general, reasonable results can be obtained by taking the cutoff to be the scale of new physics, i.e., the scale at which the effective theory is no longer valid. In our case we take this scale to be about where the technifermion structure of the technipions should become apparent, around a few TeV.

VI. $P^0 \rightarrow gg(g)$

We begin here with the results for the decays of the P^0 to two or three gluons, $\Gamma(P^0 \rightarrow gg) + \Gamma(P^0 \rightarrow ggg)$. These must be calculated together, because the two processes individually have infrared divergences. In the case of massless quarks, we must also include the diagrams of Fig. 7. For massive quarks the sum of these two decay widths is infrared finite. The result is

$$\begin{aligned}
 & \Gamma(P^0 \rightarrow gg) + \Gamma(P^0 \rightarrow ggg) \\
 &= \frac{\alpha_s \Gamma^2 M^3}{32\pi^2} C_2(G)(N^2 - 1) \\
 & \times \left[27 - \frac{65}{6}c + \frac{11}{3} \ln \frac{\mu^2}{M^2} - \frac{4}{3} \sum_f \frac{T(F)}{C_2(G)} \ln \frac{\mu^2}{2m_f^2} \right] \\
 & + \sum_f \frac{\alpha_s \Gamma G_f M m_f T(F)(N^2 - 1)}{16\pi^2} h(f). \quad (23)
 \end{aligned}$$

In (23), $\Gamma = -N_{\text{TC}} \alpha_s / 4\pi \sqrt{3} F_\pi$ (N_{TC} is the number of technicolors, and F_π is the technipion decay constant), α_s is the strong fine-structure constant, $g^2/4\pi$, and N is 3 (the number of colors in QCD). Also, M is the mass of the P^0 , μ^2 is an arbitrary mass scale introduced by the renormalization, and m_f is the mass of the quark f . The sums in (23) are over all quarks. G_f is a constant, assumed to be $\sim m_f/F_\pi$, but unknown without the details of extended technicolor interactions (or whatever mechanism one uses to give mass to fermions), and $C_2(G)$ and $T(F)$ are group-theory factors, which in our case are 3 and $\frac{1}{2}$, respectively. Finally, $h(f)$ is a function which de-

depends on the quark mass. For quarks less than half the P^0 mass ($m_f < M/2$), we get

$$h(f) = -\pi^2 + \ln^2 \left\{ \frac{4m_f^2}{M^2} / \left[1 + \left| 1 - \frac{4m_f^2}{M^2} \right| \right]^2 \right\}, \quad (24)$$

while for $m_f > M/2$, we get

$$h(f) = -\pi^2 - 4 \arctan^2 \left[\frac{4m_f^2}{M^2} - 1 \right]^{1/2} + 4\pi \arctan \left[\frac{4m_f^2}{M^2} - 1 \right]^{1/2}. \quad (25)$$

Note the absence of the parameter ϵ in (23). This quantity has no infrared divergence, and so we freely take the limit $\epsilon \rightarrow 0$.

The parameter c in (23) reflects our uncertainty in the regularization of $\epsilon^{\mu\nu\alpha\beta}$. If we take the Lorentz-noncovariant prescription, then $c=0$. If we take the covariant prescription, then $c=1$. We see that the two scenarios give results which are very similar in form, differing only in one term. However, we also see that the difference is appreciable. The dependence of the final result on the regularization of $\epsilon^{\mu\nu\alpha\beta}$ is not negligible. Henceforth, we will stick with noncovariant prescriptions of $\epsilon^{\mu\nu\alpha\beta}$ and γ_5 .

Figure 8 shows the result of our calculations for the decays $P^0 \rightarrow gg(g)$. We took the number of technicolors to be 4 and the $P^0 \bar{q}q$ coupling to be am_f/F_π , choosing $a=1$. We took α_s to be the running coupling constant

with five flavors of quarks, and evaluated it at the P^0 mass. We also set $\mu=M$. Finally, we chose $m_t=125$ GeV. Putting these values into (23) gives us the solid curve of Fig. 8.

The other two curves are the result of an attempt to separate the gluon decays into two- and three-body decays. We did this by calculating the three-gluon decay [5] with an infrared cutoff of 5 GeV in the invariant mass of any gluon system. A two-gluon system with an invariant mass of 5 GeV or more may be distinguishable from a single gluon. The dotted line in Fig. 8 represents the three-gluon decay derived in this manner. The dashed curve represents the two-gluon decay (and the three-gluon decays in which one of the gluons is soft or two of them are nearly collinear) and is obtained by subtracting the dotted line from the solid line.

The graph shows that this result is absurd above about 75 GeV. The decay rate to two gluons drops below zero at this point. As the mass of the P^0 increases, the 5-GeV cutoff goes deeper and deeper into the infrared divergence of the three-gluon decay. This causes the three-body decay width to rise rapidly, and the two-body decay width drops. We could, of course, choose a higher cutoff than 5 GeV, but this would only push the problem to a higher-mass P^0 . Of course, if we push the cutoff too high, then the entire physical meaning of the cutoff is lost, as we start to exclude events from the three-body decays which could be experimentally resolved into a three-body decay. Hence we are unable to reliably separate the gluon decays of the P^0 into three- and two-body decays.

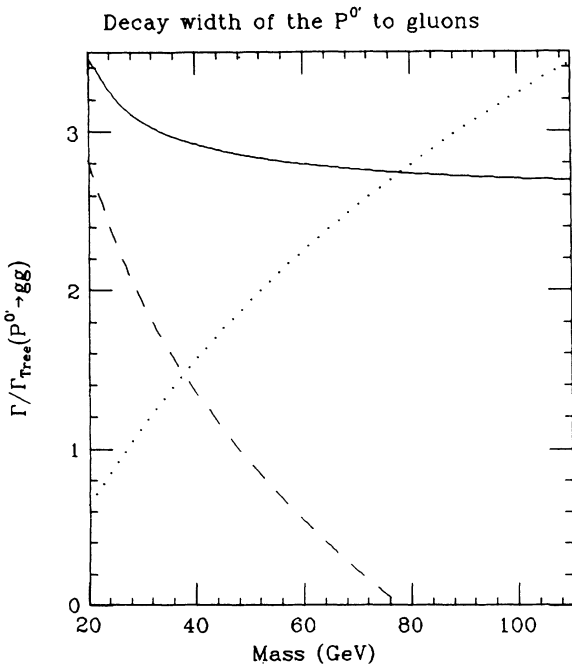


FIG. 8. Decay width of P^0 to gluons, relative to the tree-level decay. The solid line is the total, while the dashed and dotted lines are the decays to two and three gluons, respectively.

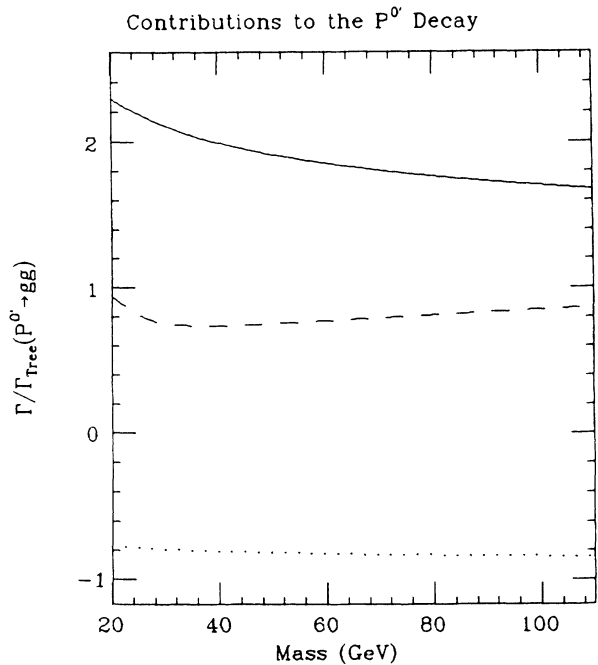


FIG. 9. Decay width of $P^0 \rightarrow gg(g)$, separated by the various virtual processes affecting the decays. The solid line is the contribution from diagrams containing only gluons. The dashed line is from the quark triangle diagrams. The dotted line is from quark loop corrections to the gluon propagator.

Figure 9 shows the $O(\alpha_s)$ corrections to the decay width of $P^{0'} \rightarrow gg$ (g), broken into three separate contributions. The first contribution (solid line) is from diagrams containing only gluons and ghosts (besides the $P^{0'}$ itself, of course). These include all the three-body decay diagrams and interference terms between the tree-level two-gluon decay and the two-body diagrams of Figs. 3(a)–3(e) (with appropriate counterterms). The second contribution (dashed line) comes from the quark triangle diagram of Fig 3(g). The final contribution (dotted line) comes from quark loop corrections to the gluon propagator [Fig. 3(f) and appropriate counterterms]. The sum of the three curves of Fig. 9 is one unit less than the solid curve of Fig. 8. The difference is that the tree-level contribution, which is 1 in our units, is included in the curves of Fig. 8.

The quark triangle contribution comes mainly from the t quark. This is especially true for higher-mass $P^{0'}$. One might expect this contribution to drop dramatically as the $P^{0'}$ mass increases. The reason for this is that widths for decays involving the $P^{0'}gg$ and $P^{0'}ggg$ vertices have a coefficient that goes as M^3 , while the overall coefficient in decays involving the $P^{0'}\bar{q}q$ vertices goes as Mm_f^2 . Hence, as M increases, the quark triangle contribution should decrease swiftly relative to the tree-level two-gluon decay and relative to all the other curves of Fig. 9. However, as the $P^{0'}$ mass increases, the virtual t quarks in the loop are closer and closer to the mass shell, which provides an enhancement, resulting in a slight overall increase in this contribution to the overall width, relative to the tree-level gluonic decay width.

In Fig. 9 the quark triangle contribution is taken to be the same sign as the tree-level contribution and the all-gluon corrections. We cannot assume that this is the case. Since G_f comes from extended technicolor and the constant Γ comes from the Wess-Zumino-Witten Lagrangian, we have no information *a priori* about the relative signs of these constants. For positive G_f we have constructive interference between the quark loop diagrams and the tree-level diagram. This is the case in the monophagic models of Ellis *et al.* [10], but we should in general also consider the case of destructive interference.

The contribution from quark loop corrections to the gluon propagator, on the other hand, is unambiguously negative. This, in fact, must be the case. In the limit of massless quarks, there is an infrared divergence in the quark loop diagrams. This infrared divergence is canceled by an infrared divergence in the square of the diagram of Fig. 7(c) for the decay $P^{0'} \rightarrow \bar{q}qg$. Since the square of this diagram must be positive and the infrared divergences must cancel, the contribution from the quark loop diagrams must be negative. Also, because of the infrared divergence in the massless-quark limit, the largest part of this contribution comes from the lightest quarks.

Because of the infrared divergence, the quark loop contribution in Fig. 9 is probably unrealistically large. Excluding all of the decay $\bar{q}qg$ of Fig. 7(c) from the two-gluon decays assumes that we can distinguish, for example, the decay $P^{0'} \rightarrow \bar{u}ug$ in which the two quarks are collinear from the decay $P^{0'} \rightarrow gg$. The u quark is simply not massive enough to allow this distinction experimentally,

and so we must also consider decays to quarks while we consider decays to gluons.

VII. TOTAL WIDTH OF THE $P^{0'}$

Considering decays to quarks as well as gluons brings on a new problem. Namely, we must now perform loop integrals and phase-space integrals in an arbitrary number of dimensions with massive particles. (Although we now have massive particles, we still have gluons, and so we still have infrared divergences to regularize.) The combined difficulties of massive particles, arbitrary number of dimensions, and lack of Lorentz covariance (we still have $\epsilon^{\mu\nu\alpha\beta}$ and γ_5 in the calculation) render the problem intractable. So now we consider the quarks to be massless, at least for the purpose of phase-space and loop integrals, except for the t quark, and we assume that the t quark is too heavy for the $P^{0'}$ to decay into. The first assumption will not hurt us much, since the $P^{0'}$ is almost certainly at least 4 times as heavy as the b quark. The second assumption is also a safe one, since the lower limit on the t -quark mass is around 85 GeV, and the $P^{0'}$ mass can only be heavier than 170 GeV through an extreme case of condensate enhancement [11–13]. Therefore, while it is not impossible that the $P^{0'}$ could decay into $\bar{t}t$ (g), it is unlikely.

One should be aware that we cannot completely assume the quarks to be massless. In the first place, the coupling $P^{0'}\bar{q}q$ is proportional to the quark mass, and so taking quarks to be massless here would eliminate many diagrams that we expect to be significant. Second, some terms which do not actually contain this coupling turn out to be proportional to the mass of a quark. We do not wish to throw these terms out. Instead, we will keep quarks massive in the coupling constant G_f ; and for other terms that are proportional to the quark mass, we will keep the lowest-order dependence on the quark mass. Effectively, this amounts to taking quarks to be massless in denominators and in the phase-space integral while keeping them massive in the numerators of expressions.

Once we decide to consider massless quarks, we of course introduce new infrared divergences, such as the divergence we just encountered which was formerly regularized by the quark mass. With the entanglement of the infrared divergences between the competing decay mechanisms, it would be a tedious business to separate each of the four decay modes $P^{0'} \rightarrow gg$, $P^{0'} \rightarrow ggg$, $P^{0'} \rightarrow \bar{q}q$, and $P^{0'} \rightarrow \bar{q}qg$. Furthermore, we have already seen that this is futile. Hence we just present the total width, first in units of the tree-level width, and then the absolute total width.

Finally, it is at this time that we must confront our remaining ultraviolet divergence, from the diagram in Fig. 6(c). Recall that this diagram has an ultraviolet divergence that was not canceled by any counterterms. Also, we opted for an ultraviolet cutoff, which we shall call Λ . The dependence on Λ will be logarithmic, and so varying Λ by a factor of 2 or so will make only a small difference. As we have mentioned, we will take Λ to be a few TeV.

We start with the amplitude for the diagram of Fig. 6(c):

$$\mathcal{M} = 2g^2 \Gamma C_2(F) \epsilon^{\mu\nu\alpha\beta} \int \frac{d^d l}{(2\pi)^d} \frac{\bar{u}(k_1) \gamma_\alpha (\not{l} + m) \gamma_\beta v(k_2) (l - k_1)_\mu (l + k_2)_\nu}{l^2 (l - k_1)^2 (l + k_2)^2}. \quad (26)$$

Next, we use Feynman parameter integrals to combine the factors in the denominator and shift the integration variable to make the denominator symmetric in l . This gives us

$$\mathcal{M} = 2g^2 \Gamma C_2(F) \epsilon^{\mu\nu\alpha\beta} \int_0^1 dx dy 2y \int \frac{d^d l}{(2\pi)^d} \left\{ \frac{\bar{u}(k_1) \gamma_\alpha \not{l} \gamma_\beta v(k_2) [l_\mu (k_1 + k_2)_\nu]}{(l^2 - Q^2)^3} - \frac{m(1-y)^2 \bar{u}(k_1) \gamma_\alpha \gamma_\beta v(k_2) k_{1\mu} k_{2\nu}}{(l^2 - Q^2)^3} \right\}, \quad (27)$$

where $Q^2 = -y^2 x(1-x)M^2$. We have now separated the ultraviolet from the infrared divergences. The first term is infrared finite, while the second term is ultraviolet finite. We now insert a factor

$$\frac{-\Lambda^2}{l^2 - \Lambda^2} \quad (28)$$

in the first term. In the limit $\Lambda \rightarrow \infty$, this factor is just 1. For finite Λ , however, this will serve to regularize the loop integral. We can then take $d=4$ in the first term as well. After that, we continue integrating in a straightforward manner.

It may seem a bit artificial inserting the factor of Eq. (28) in the middle of the calculation. If we attempt to insert the factor earlier in the calculation, however, then we cannot separate the ultraviolet from the infrared divergences. Hence it is necessary that we wait until this point in the calculation to insert the ultraviolet regularization. The rest of the calculation involves nothing new, except for the phase-space integrations, summarized in the Appendix.

Finally, we arrive at an expression for the total decay width of the $P^{0'}$ where Γ_0 is the lowest-order decay width:

$$\begin{aligned} \Gamma(P^{0'}) = & \Gamma_0(P^{0'}) + \frac{\alpha_s}{32\pi^2} \left\{ \Gamma^2(N^2 - 1) C_2(G) M^3 \left[27 + \frac{11}{3} \ln \frac{\mu^2}{M^2} \right] \right. \\ & + \Gamma^2(N^2 - 1) T(F) M^3 \left[\frac{4}{3} n_f \left[-\ln \frac{\mu^2}{M^2} + \ln 2 - \frac{53}{15} \right] - \frac{4}{3} \ln \frac{\mu^2}{2m_t^2} \right] \\ & + 2\Gamma G_t M m_t T(F) (N^2 - 1) \left[-\pi^2 - 4 \arctan^2 \left[\frac{4m_t^2}{M^2} - 1 \right]^{1/2} + 4\pi \arctan \left[\frac{4m_t^2}{M^2} - 1 \right]^{1/2} \right] \\ & \left. + \sum_f G_f^2 C_2(F) N M \left[6 \ln \frac{m_f^2}{M^2} + 25 \right] - 12 \sum_f \Gamma G_f m_f M C_2(F) N \left[\ln \frac{\Lambda^2}{M^2} + 2 \right] \right\}. \quad (29) \end{aligned}$$

The variables here are the same as in Eq. (23), with the additions that the subscript t denotes specifically the t quark, and Λ is our ultraviolet cutoff. The lowest-order decay width Γ_0 is

$$\Gamma_0(P^{0'}) = \frac{\Gamma^2 M^3}{2\pi} + \sum_f \frac{G_f^2}{8\pi} \left[M + 2 \frac{m_f^2}{M} \right] \left[1 - \frac{4m_f^2}{M^2} \right]^{1/2}. \quad (30)$$

Figure 10 shows the $O(\alpha_s)$ corrections to the decays of the $P^{0'}$ in units of the tree-level decay. The corrections are less than or about equal to the tree-level width. In obtaining the curve of Fig. 8, we used the following choices for our parameters: $N_{TC}=4$; $G_f = m_f/F_\pi$; $\alpha_s(P^2) = \alpha_s(M^2)$ for five quark flavors, so that $\alpha_s \approx 0.15$ at 50 GeV; $\mu = M$; $m_t = 125$ GeV; $F_\pi = 125$ GeV; $\Lambda = 3$ TeV.

There are two interesting characteristics to this curve. The first is that the corrections, taken as a whole, are not as large compared to the total tree-level decay as the corrections to the gluon decays were compared to the tree-level gluon decay. The reason for this is that the tree-level decays are dominated by $P^{0'} \rightarrow \bar{b}b$. Since we are dividing the corrections by the lowest-order decays, including the tree-level $\bar{b}b$ decay with these means dividing the corrections by a larger number, giving a smaller final

result than in Fig. 8. The other feature is the upward slope of the curve after about 35 GeV. This is also attributable to the tree-level decay to $\bar{b}b$, which does not climb nearly as quickly with increasing $P^{0'}$ mass as the decays involving the $P^{0'} gg$ coupling. For higher $P^{0'}$ mass, this decay ceases to dominate, and the corrections, which are dominated by the $P^{0'} gg$ coupling, increase relative to the tree-level decays.

In Fig. 11 we have plotted both the tree-level decay width and the corrections to that width, in units of MeV. We see again that the tree level dominates at low mass, but loses its dominance for higher-mass $P^{0'}$. We also see how rapidly the absolute decay width rises as a function of the $P^{0'}$ mass, increasing by roughly a full order of magnitude over the range considered.

Of course, these curves are not to be taken as a perfect description of the behavior of the $P^{0'}$. There are too

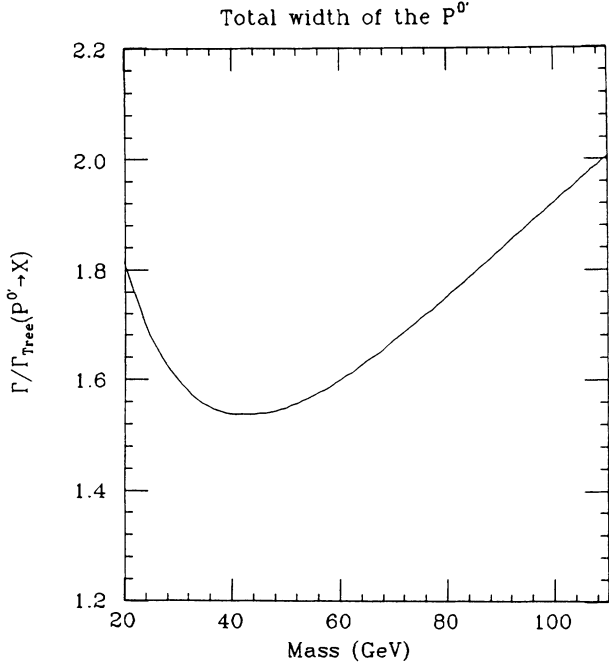


FIG. 10. Decay width of the P^0 in units of the tree-level decay width.

many uncertainties for that. We will sum them up here. First of all, the number of technicolors enters into the constant Γ in the $P^0 gg(g)$ coupling. Second, there is the parameter a in $G_f = am_f/F_\pi$, which describes the $P^0 \bar{f}f$ coupling. This uncertainty includes not only the magnitude of a , but possibly the sign as well. The quark trian-

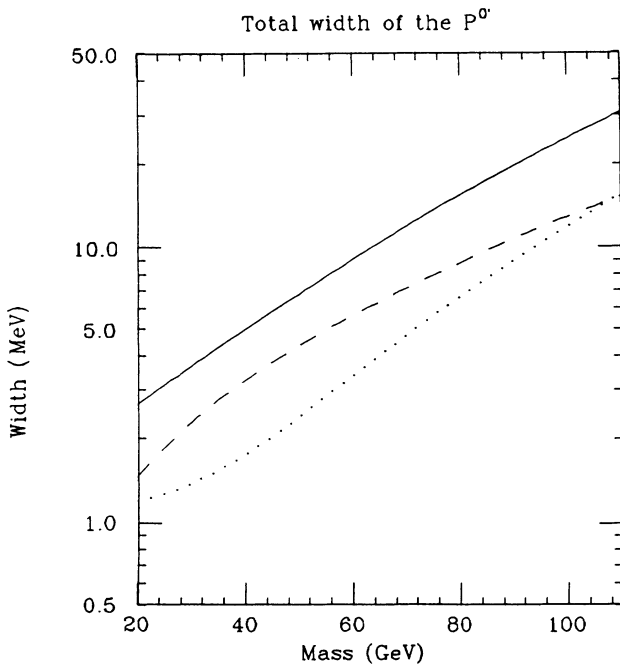


FIG. 11. Total decay width of the P^0 (solid curve) broken down into the corrections (dotted curve) and the tree-level decay width (dashed curve).

gle correction to the two-gluon decay can contribute either constructively or destructively, depending on this sign. Next, there is our choice of convention for the Levi-Civita tensor and γ_5 . Then there is our choice of both the t -quark mass and mass scale μ that we introduced in dimensional regularization. The dependence on μ can be easily seen in Eq. (29). We chose $\mu = M$. Choosing $\mu = 2M$ or $M/2$ will change the total of these corrections by only a few percent for light P^0 , up to about 10% for $M = 150$ GeV. Finally, there are, of course, higher-order corrections. Since the corrections we have calculated are sizable, we suspect that higher-order corrections may make a significant, though hopefully not overwhelming, contribution to the P^0 decay width.

The question then is, what features of our results survive these uncertainties? If a one-family technicolor model is the next correct theory of particle physics, then we can expect to see a P^0 with the following characteristics.

(i) The decay width will rise as the mass of the P^0 cubed. The rate of this rise will become very rapid as the decay becomes dominated by the $P^0 gg(g)$ couplings.

(ii) QCD corrections will be important in a perturbative approach to P^0 decays. This will be especially true for a heavy P^0 , since the tree-level $\bar{b}b$ decay (in which the corrections are smaller) will be less important in this case.

(iii) Corrections involving $P^0 \bar{q}q$ couplings will be better behaved (i.e., smaller) than corrections involving $P^0 gg(g)$ couplings. This is apparently due to the proliferation of diagrams involving the $P^0 gg(g)$ couplings, occurring because of the non-Abelian nature of QCD and, perhaps, due to the momentum dependence of the $P^0 gg(g)$ coupling. This momentum dependence may allow for a significant contribution from higher momenta in the loop integrations.

(iv) If still higher-order corrections contribute constructively to the decay width, as the next-to-lowest-order corrections have, then we can expect the curve of Fig. 11 to serve as a lower bound on the total decay width of the P^0 .

(v) For a heavy P^0 , the extended technicolor contribution (responsible for the $P^0 \bar{q}q$ coupling) will become dominated by the Wess-Zumino-Witten contribution (which gives the $P^0 gg$ couplings). In this case, then, we are mostly free from the uncertainties in the extended technicolor sector. This will not be the case, however, in the unlikely event that the P^0 will be able to decay into $\bar{t}t$.

VIII. CONCLUSIONS

Our goal in this work was twofold. First, we wanted to learn more about the properties of the technipions which are present in a technicolor theory and, in particular, of the P^0 . Second, we wanted to learn how to perform one-loop calculations in a Wess-Zumino-Witten model in which a non-Abelian subgroup of the chiral symmetry is gauged. This second goal was, in fact, necessary in order to accomplish our first goal.

We discovered several things about performing these one-loop calculations. First, we know that on-shell re-

normalization is inappropriate for such a calculation, because of the presence of infrared divergences. In order for the infrared divergences to cancel, we require a renormalization scheme in which the coupling-constant renormalization constant (Z_g in our notation) contains no infrared divergence. This is not the case in on-shell renormalization, and so we used modified minimal subtraction ($\overline{\text{MS}}$), in which none of the renormalization constants contain infrared divergences. Second, we learned that use of a gluon cutoff to regularize the infrared divergences is also inappropriate, since in the end the divergences will not cancel. The trouble is attributed to the trilinear coupling of gluons. This led us to use dimensional regularization to regularize the infrared as well as the ultraviolet divergences. Third, we found that if we interpret the quantities in the Wess-Zumino-Witten Lagrangian correctly as bare quantities, then almost all of the ultraviolet divergences in the process that we have considered can be eliminated through very straightforward renormalization. (In fact, almost all the renormalization necessary is just the usual renormalization of QCD.)

Finally, we found that we are left with a choice in our handling of the quantities $\epsilon^{\mu\nu\alpha\beta}$ and γ_5 in dimensional regularization. We can obtain an answer equally well by treating these quantities as Lorentz-covariant or noncovariant quantities. In either case the infrared divergences cancel, but the answer one obtains can differ appreciably between the two prescriptions. In the end we chose the noncovariant scheme, since our best indication from other work is that this scheme is more appropriate for the Wess-Zumino-Witten model.

We eventually obtained results in our calculation of the P^0 , which were presented in the preceding section. The $O(\alpha_s)$ corrections to the decays of the P^0 are quite large relative to the tree-level values, although the total width is still small. Our final expression for the total width of the P^0 is probably a good lower bound for the width, although higher-order corrections may be important as well. There is a great deal of model dependence in the result. Finally, we attempted to separate the width into its various decay modes. This proved futile because of the combination of the strength of the coupling and infrared divergences associated with massless gluons and light quarks.

APPENDIX

We have chosen dimensional regularization to regularize the infrared divergences in our calculation, and so we need to know how to perform phase-space integration in d dimensions. This is not difficult in the case of massless particles in the final state and a Lorentz-covariant integrand [14]. It becomes much more difficult if the integrand is not covariant.

Two-body phase space

In d dimensions two-body phase space takes on the form

$$(\mu^2)^{2-d/2} \frac{d^{d-1}k_1}{(2\pi)^{d-1}2E_1} \frac{d^{d-1}k_2}{(2\pi)^{d-1}2E_2} (2\pi)^d \delta^d(P - k_1 - k_2), \quad (\text{A1})$$

where we can substitute at will

$$\frac{d^{d-1}k}{2E} \rightleftharpoons d^d k \delta(k^2), \quad (\text{A2})$$

and we have assumed that the particles are massless. The parameter μ^2 keeps the integral at a constant-mass dimension.

In d -dimensional space-time,

$$d^{d-2}\Omega = \sin^{d-3}\theta_1 \sin^{d-4}\theta_2 \cdots \sin\theta_{d-3} d\theta_1 d\theta_2 \cdots d\theta_{d-2}. \quad (\text{A3})$$

The ranges of the angles in (A3) are from 0 to π except for θ_{d-2} , which runs from 0 to 2π . The integration can be performed with the help of the identity

$$\int_0^{\pi/2} \cos^m \theta \sin^n \theta d\theta = \frac{1}{2} B\left[\frac{m+1}{2}, \frac{n+1}{2}\right], \quad (\text{A4})$$

where $B(a, b)$ is the beta function,

$$B(a, b) = \frac{\Gamma(a)\Gamma(b)}{\Gamma(a+b)}. \quad (\text{A5})$$

In addition, we can use the identity

$$\Gamma\left[a + \frac{1}{2}\right] = \frac{\sqrt{\pi}\Gamma(2a)}{2^{2a-1}\Gamma(a)} \quad (\text{A6})$$

to express gamma functions with half-integer arguments in terms of gamma functions with integer arguments.

We can, in fact, finish the phase-space integration if there is no angular dependence. The result of this is

$$\frac{1}{8\pi} \left[\frac{4\pi\mu^2}{P^2} \right]^\epsilon \frac{\Gamma(1-\epsilon)}{\Gamma(2-2\epsilon)}. \quad (\text{A7})$$

We see the four-dimensional result reproduced as $\epsilon \rightarrow 0$.

We are especially interested, however, in the case where the integrand is *not* Lorentz covariant. The noncovariant prescription for the dimensional regularization of $\epsilon^{\mu\nu\alpha\beta}$ leads to terms in the integrand such as \underline{k}_1^2 and $\underline{k}_1 \cdot \underline{k}_2$, which are the products of d -dimensional vectors truncated to four dimensions.

To handle this case, we start by integrating k_2 . We use the substitution (A2) with the momentum k_2 and integrate $d^d k_2$ with the δ function. This gives us

$$\frac{d^{d-1}k_1}{(2\pi)^{d-2}2E_1} \delta[(P - k_1)^2]. \quad (\text{A8})$$

For convenience, we will work in the center of mass and in units where $P^2 = 1$, so that $P = (1, 0, 0, \dots)$. The noncovariant quantities that we will have to worry about are just \underline{k}_1^2 , \underline{P}^2 , and $\underline{P} \cdot \underline{k}_1$. (Remember, we have integrated k_2 already.) But in the center of mass, the last two quantities are just $P_0^2 = 1$ and $P_0 E_1 = E_1$. Hence the only non-

covariant quantity in our integrand will be \underline{k}_1^2 . Phase space has now become

$$\frac{d^{d-1}k_1}{(2\pi)^{d-2}2E_1} \delta(1-2E_1)|\mathcal{M}|^2, \quad (\text{A9})$$

$$k_1 = (E_1, \underline{K} \cos\theta_1, \underline{K} \sin\theta_1 \cos\theta_2, \underline{K} \sin\theta_1 \sin\theta_2, \underline{K} \cos\phi_1, \underline{K} \sin\phi_1 \cos\phi_2, \dots, \underline{K} \sin\phi_1 \cdots \sin\phi_{d-5}), \quad (\text{A10})$$

where $E_1^2 = \underline{K}^2 + \underline{K}^2$. Then we make the change

$$\begin{aligned} \underline{K} &= E_1 \cos\alpha, \\ \underline{K} &= E_1 \sin\alpha. \end{aligned} \quad (\text{A11})$$

Then the integration measure for k_1 is

$$d^{d-1}k_1 = E_1^{d-2} dE_1 \cos^2\alpha \sin^{d-5}\alpha d\alpha \sin\theta_1 d\theta_1 d\theta_2 \sin^{d-6}\phi_1 \sin^{d-7}\phi_2 \cdots \sin\phi_{d-6} d\phi_1 \cdots d\phi_{d-5}. \quad (\text{A12})$$

In this parametrization,

$$\underline{k}_1^2 = E_1^2(1 - \cos^2\alpha) = E_1^2 \sin^2\alpha. \quad (\text{A13})$$

Hence we can integrate all of the θ and ϕ variables immediately using the identity (A4), because the integrand depends only on E_1 and α . The α integral is done using (A4) as well, and the E_1 integral is done with the δ function.

Three-body phase space

Three-body phase space in d dimensions requires a few more tricks. We start with

$$(\mu^2)^{2e} \frac{d^{d-1}k_1}{(2\pi)^{d-1}2E_1} \frac{d^{d-1}k_2}{(2\pi)^{d-1}2E_2} \frac{d^d k_3}{(2\pi)^{d-1}} \delta(k_3^2) (2\pi)^d \delta^d(P - k_1 - k_2 - k_3) |\mathcal{M}|^2. \quad (\text{A14})$$

Integrating k_3 , we get

$$(\mu^2)^{2e} \frac{d^{d-1}k_1 d^{d-1}k_2}{(2\pi)^{2d-3} 2E_1 2E_2} \delta[(P - k_1 - k_2)^2] |\mathcal{M}|^2. \quad (\text{A15})$$

Again, we work in the center of mass and take $P^2 = 1$. Also, we define

$$x_i = 2P \cdot k_i, \quad (\text{A16})$$

where i can be 1, 2, or 3. Then $E_i = x_i/2$ in the center of mass. This gives us

$$(\mu^2)^{2e} \frac{d^{d-1}k_1 d^{d-1}k_2}{(2\pi)^{2d-3} x_1 x_2} \delta[(1 - x_1 - x_2) + 2k_1 \cdot k_2] |\mathcal{M}|^2. \quad (\text{A17})$$

Next, we switch to polar coordinates. We will use θ_i to denote angles in k_1 and ψ_i to denote angles in k_2 . If our integrand is Lorentz covariant, then our next trick is to perform a coordinate transformation on the spatial components of k_2 , such that in terms of the new coordinates k'_2 ,

$$k_1 \cdot k'_2 = E_1 E_2 (1 - \cos\psi_1) = \frac{1}{4} x_1 x_2 (1 - \cos\psi_1),$$

while k_1^2 and k_2^2 remain unchanged.¹ We can then use the

¹It is best not to think of this as a rotation. Under a rotation the product $k_1 \cdot k_2$ is an invariant. This is simply a series of variable changes on $(k_2, \dots, k_{2,d-1})$ with Jacobian 1.

where we have now included the square of the amplitude.

We now choose a parametrization for k_1 which will make \underline{k}_1^2 take on a simple form. First, we separate the real four dimensions of k_1 from the extra dimensions and put each set of dimensions into polar coordinates:

remaining δ function to integrate ψ_1 . However, we have noncovariant quantities such as \underline{k}_2^2 and $\underline{k}_1 \cdot \underline{k}_2$, and these quantities are not invariant under such a transformation. We can still make the transformation, but we must now see how these quantities are affected.

We can start out by making transformations among the first three spatial components of k_2 and among the last $d-4$ components with impunity, so that all of the relevant quantities in $|\mathcal{M}|^2$ are left unchanged, except that

$$k_1 \cdot k_2 = E_1 E_2 - \underline{K}_1 k_{21} - \underline{K}_1 k_{24} \quad (\text{A18})$$

and

$$\underline{k}_1 \cdot \underline{k}_2 = E_1 E_2 - \underline{K}_1 k_{21}, \quad (\text{A19})$$

where k_{ij} is the j th spatial component of k_2 . Also, $\underline{K}_i^2 = k_{i1}^2 + k_{i2}^2 + k_{i3}^2$ and $\underline{K}_i^2 = k_{i4}^2 + k_{i5}^2 + \dots$, so that $E_i^2 = \underline{K}_i^2 + \underline{K}_i^2$. The other kinematic factors we have to deal with are

$$\begin{aligned} \underline{k}_1^2 &= E_1^2 - \underline{K}_1^2, \\ \underline{k}_2^2 &= E_2^2 - \underline{K}_2^2. \end{aligned} \quad (\text{A20})$$

The last transformation we make is

$$\begin{pmatrix} k_{21} \\ k_{24} \end{pmatrix} = \frac{1}{E_1} \begin{pmatrix} \underline{K}_1 & -\underline{K}_1 \\ \underline{K}_1 & \underline{K}_1 \end{pmatrix} \begin{pmatrix} k'_{21} \\ k'_{24} \end{pmatrix}. \quad (\text{A21})$$

Finally, we switch to polar coordinates in k_2 and we treat

k_1 just as we did in the two-body case, going to polar coordinates separately in the first three spatial components and the last $d-4$ components. Then the kinematic factors in the integrand become

$$k_1 \cdot k_2 = E_1 E_2 (1 - \cos \psi_1), \quad (\text{A22})$$

$$\underline{k}_1 \cdot \underline{k}_2 = E_1 E_2 (1 - \cos^2 \alpha \cos \psi_1 + \cos \alpha \sin \alpha \sin \psi_1 \sin \psi_2 \sin \psi_3 \cos \psi_4), \quad (\text{A23})$$

$$\underline{k}_1^2 = E_1^2 \sin^2 \alpha, \quad (\text{A24})$$

$$\begin{aligned} \underline{k}_2^2 = E_2^2 & (\sin^2 \psi_1 \sin^2 \psi_2 \sin^2 \psi_3 + \sin^2 \alpha \cos^2 \psi_1 \\ & + 2 \cos \alpha \sin \alpha \cos \psi_1 \sin \psi_1 \sin \psi_2 \sin \psi_3 \cos \psi_4 \\ & - \sin^2 \alpha \sin^2 \psi_1 \sin^2 \psi_2 \sin^2 \psi_3 \cos^2 \psi_4). \end{aligned} \quad (\text{A25})$$

Recall that ψ_i is the i th angle describing k_2 and that $\cos \alpha$ describes that fraction of \mathbf{k}_1 which lies in the three physical spatial dimensions.

Any angle not appearing in (A22)–(A25) can be integrated immediately. We can also replace the E 's with $\frac{1}{2}x$'s. We integrate ψ_1 with the δ function left over from the k_3 integration. Then we make one last variable change, trading in the variable x_2 for v , where $x_2 = 1 - vx_1$. Finally, we get

$$\frac{2^{2\epsilon}}{64\pi^{9/2}} (4\pi\mu^2)^{2\epsilon} \frac{1}{\Gamma(-\epsilon)\Gamma(-\frac{1}{2}-\epsilon)} x_1^{1-2\epsilon} (1-x_1)^{-\epsilon} v^{-\epsilon} (1-v)^{-\epsilon} dx_1 dv \times \cos^2 \alpha \sin^{d-5} \alpha d\alpha \sin^{d-4} \psi_2 \sin^{d-4} \psi_3 \sin^{d-6} \psi_4 d\psi_2 d\psi_3 d\psi_4. \quad (\text{A26})$$

The x_1 and v integrations can be performed using the identity

$$\int_0^1 da a^m (1-a)^n = B(m+1, n+1), \quad (\text{A27})$$

and the angular integrations can be done with (A4) and (A6). We have now covered everything we need to know to do the phase-space integrations for the processes in this work.

[1] J. Wess and B. Zumino, *Phys. Lett.* **37B**, 95 (1971).

[2] E. Witten, *Nucl. Phys.* **B223**, 422 (1983).

[3] S. Weinberg, *Phys. Rev. D* **19**, 1277 (1979); L. Susskind, *ibid.* **20**, 2619 (1979); E. Farhi and L. Susskind, *Phys. Rep.* **74**, 277 (1981).

[4] Ö. Kaymakçalan, S. Rajeev, and J. Schechter, *Phys. Rev. D* **30**, 594 (1984).

[5] D. McKay, D. Slaven, and B.-L. Young, *Phys. Rev. D* **34**, 3394 (1986); W.-C. Kuo, D. McKay, and B.-L. Young, *ibid.* **36**, 2729 (1987).

[6] S. Dimopoulos and L. Susskind, *Nucl. Phys.* **B155**, 237 (1979); E. Eichten and K. Lane, *Phys. Lett.* **90B**, 125 (1980).

[7] Y.-P. Yao, *Phys. Rev. Lett.* **36**, 653 (1976).

[8] A. Sugamoto, *Phys. Rev. D* **16**, 1065 (1977).

[9] M. Bos, *Ann. Phys. (N.Y.)* **181**, 177 (1988).

[10] J. Ellis, M. K. Gaillard, D. V. Nanopoulos, and P. Sikivie, *Nucl. Phys.* **B183**, 529 (1981).

[11] T. Appelquist and L. C. R. Wijewardhana, *Phys. Rev. D* **36**, 568 (1987).

[12] B. Holdom, *Phys. Rev. D* **24**, 1441 (1981); K. Yamawaki, M. Bando, and K. Matumoto, *Phys. Rev. Lett.* **56**, 1335 (1986).

[13] T. Appelquist, M. Einhorn, T. Takeuchi, and L. C. R. Wijewardhana, *Phys. Lett. B* **220**, 223 (1989).

[14] R. Field, *Applications of Perturbative QCD* (Addison-Wesley, Reading, MA, 1989).